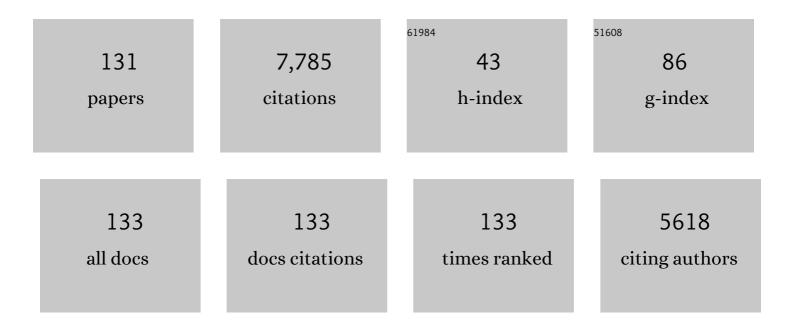
Jochem Verrelst

List of Publications by Year in descending order

Source: https://exaly.com/author-pdf/5417089/publications.pdf Version: 2024-02-01



#	Article	IF	CITATIONS
1	Systematic Assessment of MODTRAN Emulators for Atmospheric Correction. IEEE Transactions on Geoscience and Remote Sensing, 2022, 60, 1-17.	6.3	11
2	Quantifying Fundamental Vegetation Traits over Europe Using the Sentinel-3 OLCI Catalogue in Google Earth Engine. Remote Sensing, 2022, 14, 1347.	4.0	9
3	Retrieval of Crop Variables from Proximal Multispectral UAV Image Data Using PROSAIL in Maize Canopy. Remote Sensing, 2022, 14, 1247.	4.0	16
4	Quantifying mangrove leaf area index from Sentinel-2 imagery using hybrid models and active learning. International Journal of Remote Sensing, 2022, 43, 5636-5657.	2.9	11
5	Evaluation of Hybrid Models to Estimate Chlorophyll and Nitrogen Content of Maize Crops in the Framework of the Future CHIME Mission. Remote Sensing, 2022, 14, 1792.	4.0	17
6	Multi-Season Phenology Mapping of Nile Delta Croplands Using Time Series of Sentinel-2 and Landsat 8 Green LAI. Remote Sensing, 2022, 14, 1812.	4.0	8
7	Hybrid retrieval of crop traits from multi-temporal PRISMA hyperspectral imagery. ISPRS Journal of Photogrammetry and Remote Sensing, 2022, 187, 362-377.	11.1	37
8	Gaussian processes retrieval of crop traits in Google Earth Engine based on Sentinel-2 top-of-atmosphere data. Remote Sensing of Environment, 2022, 273, 112958.	11.0	32
9	Monitoring Cropland Phenology on Google Earth Engine Using Gaussian Process Regression. Remote Sensing, 2022, 14, 146.	4.0	28
10	Trends in Satellite Sensors and Image Time Series Processing Methods for Crop Phenology Monitoring. Springer Optimization and Its Applications, 2022, , 199-231.	0.9	3
11	Prototyping Crop Traits Retrieval Models for CHIME: Dimensionality Reduction Strategies Applied to PRISMA Data. Remote Sensing, 2022, 14, 2448.	4.0	16
12	Estimating soil moisture content under grassland with hyperspectral data using radiative transfer modelling and machine learning. International Journal of Applied Earth Observation and Geoinformation, 2022, 110, 102817.	1.9	2
13	Improving the remote estimation of soil organic carbon in complex ecosystems with Sentinel-2 and GIS using Gaussian processes regression. Plant and Soil, 2022, 479, 159-183.	3.7	13
14	Intelligent Sampling for Vegetation Nitrogen Mapping Based on Hybrid Machine Learning Algorithms. IEEE Geoscience and Remote Sensing Letters, 2021, 18, 2038-2042.	3.1	43
15	Prototyping Sentinel-2 green LAI and brown LAI products for cropland monitoring. Remote Sensing of Environment, 2021, 255, 112168.	11.0	37
16	Denoising AVIRIS-NG Data for Generation of New Chlorophyll Indices. IEEE Sensors Journal, 2021, 21, 6982-6989.	4.7	13
17	Potential use of grapevine cv Askari for heavy metal phytoremediation purposes at greenhouse scale. Environmental Science and Pollution Research, 2021, 28, 12447-12458.	5.3	5
18	A Survey of Active Learning for Quantifying Vegetation Traits from Terrestrial Earth Observation Data. Remote Sensing, 2021, 13, 287.	4.0	51

#	Article	IF	CITATIONS
19	Hybrid inversion of radiative transfer models based on high spatial resolution satellite reflectance data improves fractional vegetation cover retrieval in heterogeneous ecological systems after fire. Remote Sensing of Environment, 2021, 255, 112304.	11.0	26
20	Comparison of Crop Trait Retrieval Strategies Using UAV-Based VNIR Hyperspectral Imaging. Remote Sensing, 2021, 13, 1748.	4.0	26
21	Top-of-Atmosphere Retrieval of Multiple Crop Traits Using Variational Heteroscedastic Gaussian Processes within a Hybrid Workflow. Remote Sensing, 2021, 13, 1589.	4.0	28
22	Retrieving and Validating Leaf and Canopy Chlorophyll Content at Moderate Resolution: A Multiscale Analysis with the Sentinel-3 OLCI Sensor. Remote Sensing, 2021, 13, 1419.	4.0	14
23	Crop Nitrogen Retrieval Methods for Simulated Sentinel-2 Data Using In-Field Spectrometer Data. Remote Sensing, 2021, 13, 2404.	4.0	10
24	Mapping landscape canopy nitrogen content from space using PRISMA data. ISPRS Journal of Photogrammetry and Remote Sensing, 2021, 178, 382-395.	11.1	45
25	Classification of Plant Ecological Units in Heterogeneous Semi-Steppe Rangelands: Performance Assessment of Four Classification Algorithms. Remote Sensing, 2021, 13, 3433.	4.0	3
26	Estimating the phenological dynamics of irrigated rice leaf area index using the combination of PROSAIL and Gaussian Process Regression. International Journal of Applied Earth Observation and Geoinformation, 2021, 102, 102454.	2.8	9
27	Green LAI Mapping and Cloud Gap-Filling Using Gaussian Process Regression in Google Earth Engine. Remote Sensing, 2021, 13, 403.	4.0	42
28	Crop Phenology Retrieval Through Gaussian Process Regression. , 2021, , .		0
29	Emulation of Sun-Induced Fluorescence from Radiance Data Recorded by the HyPlant Airborne Imaging Spectrometer. Remote Sensing, 2021, 13, 4368.	4.0	7
30	Vegetation Types Mapping Using Multi-Temporal Landsat Images in the Google Earth Engine Platform. Remote Sensing, 2021, 13, 4683.	4.0	8
31	Assessing Non-Photosynthetic Cropland Biomass from Spaceborne Hyperspectral Imagery. Remote Sensing, 2021, 13, 4711.	4.0	16
32	Remote sensing algorithms for estimation of fractional vegetation cover using pure vegetation index values: A review. ISPRS Journal of Photogrammetry and Remote Sensing, 2020, 159, 364-377.	11.1	187
33	Estimation of leaf area index using PROSAIL based LUT inversion, MLRA-GPR and empirical models: Case study of tropical deciduous forest plantation, North India. International Journal of Applied Earth Observation and Geoinformation, 2020, 86, 102027.	2.8	30
34	Transboundary Basins Need More Attention: Anthropogenic Impacts on Land Cover Changes in Aras River Basin, Monitoring and Prediction. Remote Sensing, 2020, 12, 3329.	4.0	13
35	Quantifying vegetation biophysical variables from the Sentinel-3/FLEX tandem mission: Evaluation of the synergy of OLCI and FLORIS data sources. Remote Sensing of Environment, 2020, 251, 112101.	11.0	39
36	Gaussian processes retrieval of LAI from Sentinel-2 top-of-atmosphere radiance data. ISPRS Journal of Photogrammetry and Remote Sensing, 2020, 167, 289-304.	11.1	43

#	Article	IF	CITATIONS
37	Urban Heat Island Monitoring and Impacts on Citizen's General Health Status in Isfahan Metropolis: A Remote Sensing and Field Survey Approach. Remote Sensing, 2020, 12, 1350.	4.0	54
38	Partitioning net carbon dioxide fluxes into photosynthesis and respiration using neural networks. Global Change Biology, 2020, 26, 5235-5253.	9.5	42
39	Retrieval of aboveground crop nitrogen content with a hybrid machine learning method. International Journal of Applied Earth Observation and Geoinformation, 2020, 92, 102174.	2.8	70
40	Comparative analysis of atmospheric radiative transfer models using the Atmospheric Look-up table Generator (ALG) toolbox (version 2.0). Geoscientific Model Development, 2020, 13, 1945-1957.	3.6	20
41	Crop nitrogen monitoring: Recent progress and principal developments in the context of imaging spectroscopy missions. Remote Sensing of Environment, 2020, 242, 111758.	11.0	183
42	Assessment of Workflow Feature Selection on Forest LAI Prediction with Sentinel-2A MSI, Landsat 7 ETM+ and Landsat 8 OLI. Remote Sensing, 2020, 12, 915.	4.0	41
43	Optimal Spectral Wavelengths for Discriminating Orchard Species Using Multivariate Statistical Techniques. Remote Sensing, 2020, 12, 63.	4.0	4
44	DATimeS: A machine learning time series GUI toolbox for gap-filling and vegetation phenology trends detection. Environmental Modelling and Software, 2020, 127, 104666.	4.5	44
45	Statistical biophysical parameter retrieval and emulation with Gaussian processes. Data Handling in Science and Technology, 2020, 32, 333-368.	3.1	0
46	Optimizing Gaussian Process Regression for Image Time Series Gap-Filling and Crop Monitoring. Agronomy, 2020, 10, 618.	3.0	23
47	Quantifying Vegetation Biophysical Variables from Imaging Spectroscopy Data: A Review on Retrieval Methods. Surveys in Geophysics, 2019, 40, 589-629.	4.6	265
48	Exploring the spatial relationship between airborne-derived red and far-red sun-induced fluorescence and process-based GPP estimates in a forest ecosystem. Remote Sensing of Environment, 2019, 231, 111272.	11.0	34
49	Fusing optical and SAR time series for LAI gap filling with multioutput Gaussian processes. Remote Sensing of Environment, 2019, 235, 111452.	11.0	64
50	Quantifying the Robustness of Vegetation Indices through Global Sensitivity Analysis of Homogeneous and Forest Leaf-Canopy Radiative Transfer Models. Remote Sensing, 2019, 11, 2418.	4.0	36
51	Biomass Assessment of Agricultural Crops Using Multi-temporal Dual-Polarimetric TerraSAR-X Data. PFG - Journal of Photogrammetry, Remote Sensing and Geoinformation Science, 2019, 87, 159-175.	1.1	5
52	Global Sensitivity Analysis of Leaf-Canopy-Atmosphere RTMs: Implications for Biophysical Variables Retrieval from Top-of-Atmosphere Radiance Data. Remote Sensing, 2019, 11, 1923.	4.0	37
53	Variability and Uncertainty Challenges in Scaling Imaging Spectroscopy Retrievals and Validations from Leaves Up to Vegetation Canopies. Surveys in Geophysics, 2019, 40, 631-656.	4.6	35
54	Scenario-based discrimination of common grapevine varieties using in-field hyperspectral data in the western of Iran. International Journal of Applied Earth Observation and Geoinformation, 2019, 80, 26-37.	2.8	14

#	Article	IF	CITATIONS
55	Approximating Empirical Surface Reflectance Data through Emulation: Opportunities for Synthetic Scene Generation. Remote Sensing, 2019, 11, 157.	4.0	10
56	Gradient-Based Automatic Lookup Table Generator for Radiative Transfer Models. IEEE Transactions on Geoscience and Remote Sensing, 2019, 57, 1040-1048.	6.3	15
57	Eco-Friendly Estimation of Heavy Metal Contents in Grapevine Foliage Using In-Field Hyperspectral Data and Multivariate Analysis. Remote Sensing, 2019, 11, 2731.	4.0	15
58	Design of a Generic 3-D Scene Generator for Passive Optical Missions and Its Implementation for the ESA's FLEX/Sentinel-3 Tandem Mission. IEEE Transactions on Geoscience and Remote Sensing, 2018, 56, 1290-1307.	6.3	16
59	Retrieval of canopy water content of different crop types with two new hyperspectral indices: Water Absorption Area Index and Depth Water Index. International Journal of Applied Earth Observation and Geoinformation, 2018, 67, 69-78.	2.8	44
60	Advances in Kernel Machines for Image Classification and Biophysical Parameter Retrieval. Signals and Communication Technology, 2018, , 399-441.	0.5	2
61	FLEX/S3 Tandem Mission Performance Assessment: Evolution of the End-to-End Simulator Flex-E. , 2018, , .		Ο
62	Alg: a Toolbox for the Generation of Look-Up tables Based on Atmospheric Radiative Transfer Models. , 2018, , .		0
63	Compensation of Oxygen Transmittance Effects for Proximal Sensing Retrieval of Canopy–Leaving Sun–Induced Chlorophyll Fluorescence. Remote Sensing, 2018, 10, 1551.	4.0	44
64	Approximating Experimental Vegetation Spectroscopy Data through Emulation. , 2018, , .		0
65	Statistical Learning For End-To-End Simulations. , 2018, , .		0
66	The Sensagri Sentinel-2 Lai Green and Brown Product: from Algorithm Development Towards Operational Mapping. , 2018, , .		1
67	Progress in Emulation For Radiative Transfer Modeling And Mapping. , 2018, , .		1
68	Remote Estimation of Canopy Water Content in Different Crop Types with New Hyperspectral Indices. , 2018, , .		0
69	Emulation as an Accurate Alternative to Interpolation in Sampling Radiative Transfer Codes. IEEE Journal of Selected Topics in Applied Earth Observations and Remote Sensing, 2018, 11, 4918-4931.	4.9	25
70	Hyperspectral dimensionality reduction for biophysical variable statistical retrieval. ISPRS Journal of Photogrammetry and Remote Sensing, 2017, 132, 88-101.	11.1	86
71	Impact of Atmospheric Inversion Effects on Solar-Induced Chlorophyll Fluorescence: Exploitation of the Apparent Reflectance as a Quality Indicator. Remote Sensing, 2017, 9, 622.	4.0	20
72	Assessment of Approximations in Aerosol Optical Properties and Vertical Distribution into FLEX Atmospherically-Corrected Surface Reflectance and Retrieved Sun-Induced Fluorescence. Remote Sensing, 2017, 9, 675.	4.0	12

#	Article	IF	CITATIONS
73	SCOPE-Based Emulators for Fast Generation of Synthetic Canopy Reflectance and Sun-Induced Fluorescence Spectra. Remote Sensing, 2017, 9, 927.	4.0	41
74	A Global Sensitivity Analysis Toolbox to Quantify Drivers of Vegetation Radiative Transfer Models. , 2017, , 319-339.		5
75	Oxygen transmittance correction for solar-induced chlorophyll fluorescence measured on proximal sensing: Application to the NASA-GSFC fusion tower. , 2017, , .		2
76	Emulation of Leaf, Canopy and Atmosphere Radiative Transfer Models for Fast Global Sensitivity Analysis. Remote Sensing, 2016, 8, 673.	4.0	73
77	FLEX End-to-End Mission Performance Simulator. IEEE Transactions on Geoscience and Remote Sensing, 2016, 54, 4215-4223.	6.3	42
78	Spectral band selection for vegetation properties retrieval using Gaussian processes regression. International Journal of Applied Earth Observation and Geoinformation, 2016, 52, 554-567.	2.8	125
79	Learning Structures in Earth Observation Data with Gaussian Processes. Lecture Notes in Computer Science, 2016, , 78-94.	1.3	0
80	A Survey on Gaussian Processes for Earth-Observation Data Analysis: A Comprehensive Investigation. IEEE Geoscience and Remote Sensing Magazine, 2016, 4, 58-78.	9.6	172
81	Active Learning Methods for Efficient Hybrid Biophysical Variable Retrieval. IEEE Geoscience and Remote Sensing Letters, 2016, 13, 1012-1016.	3.1	60
82	Evaluating the predictive power of sun-induced chlorophyll fluorescence to estimate net photosynthesis of vegetation canopies: A SCOPE modeling study. Remote Sensing of Environment, 2016, 176, 139-151.	11.0	111
83	Biophysical parameter retrieval with warped Gaussian processes. , 2015, , .		1
84	A sun-induced vegetation fluorescence retrieval method from top of atmosphere radiance for the FLEX/Sentinel-3 TanDEM mission. , 2015, , .		1
85	Sunâ€induced fluorescence – a new probe of photosynthesis: First maps from the imaging spectrometerÂ <i>HyPlant</i> . Global Change Biology, 2015, 21, 4673-4684.	9.5	213
86	An Emulator Toolbox to Approximate Radiative Transfer Models with Statistical Learning. Remote Sensing, 2015, 7, 9347-9370.	4.0	61
87	Replacing radiative transfer models by surrogate approximations through machine learning. , 2015, , .		4
88	Global sensitivity analysis of the SCOPE model: What drives simulated canopy-leaving sun-induced fluorescence?. Remote Sensing of Environment, 2015, 166, 8-21.	11.0	211
89	Optical remote sensing and the retrieval of terrestrial vegetation bio-geophysical properties – A review. ISPRS Journal of Photogrammetry and Remote Sensing, 2015, 108, 273-290.	11.1	482
90	Experimental Sentinel-2 LAI estimation using parametric, non-parametric and physical retrieval methods – A comparison. ISPRS Journal of Photogrammetry and Remote Sensing, 2015, 108, 260-272.	11.1	267

#	Article	IF	CITATIONS
91	Leaf reflectance variation along a vertical crown gradient of two deciduous tree species in a Belgian industrial habitat. Environmental Pollution, 2015, 204, 324-332.	7.5	3
92	Bidirectional sun-induced chlorophyll fluorescence emission is influenced by leaf structure and light scattering properties — A bottom-up approach. Remote Sensing of Environment, 2015, 158, 169-179.	11.0	99
93	Brown and green LAI mapping through spectral indices. International Journal of Applied Earth Observation and Geoinformation, 2015, 35, 350-358.	2.8	61
94	Análisis de métodos de validación cruzada para la obtención robusta de parámetros biofÃsicos. Revista De Teledeteccion, 2015, , 55.	0.6	7
95	A fluorescence retrieval method for the flex sentinel-3 tandem mission. , 2014, , .		0
96	On the Semi-Automatic Retrieval of Biophysical Parameters Based on Spectral Index Optimization. Remote Sensing, 2014, 6, 4927-4951.	4.0	75
97	A Comparison of Advanced Regression Algorithms for Quantifying Urban Land Cover. Remote Sensing, 2014, 6, 6324-6346.	4.0	30
98	Chlorophyll content mapping of urban vegetation in the city of Valencia based on the hyperspectral NAOC index. Ecological Indicators, 2014, 40, 34-42.	6.3	32
99	Mapping a priori defined plant associations using remotely sensed vegetation characteristics. Remote Sensing of Environment, 2014, 140, 639-651.	11.0	21
100	Optimizing LUT-Based RTM Inversion for Semiautomatic Mapping of Crop Biophysical Parameters from Sentinel-2 and -3 Data: Role of Cost Functions. IEEE Transactions on Geoscience and Remote Sensing, 2014, 52, 257-269.	6.3	97
101	Retrieval of Biophysical Parameters With Heteroscedastic Gaussian Processes. IEEE Geoscience and Remote Sensing Letters, 2014, 11, 838-842.	3.1	94
102	A field study on solar-induced chlorophyll fluorescence and pigment parameters along a vertical canopy gradient of four tree species in an urban environment. Science of the Total Environment, 2014, 466-467, 185-194.	8.0	25
103	Gaussian processes retrieval of leaf parameters from a multi-species reflectance, absorbance and fluorescence dataset. Journal of Photochemistry and Photobiology B: Biology, 2014, 134, 37-48.	3.8	70
104	Toward a Semiautomatic Machine Learning Retrieval of Biophysical Parameters. IEEE Journal of Selected Topics in Applied Earth Observations and Remote Sensing, 2014, 7, 1249-1259.	4.9	98
105	Global sensitivity analysis of the A-SCOPE model in support of future FLEX fluorescence retrievals. , 2014, , .		0
106	Sensitivity of scope modelled GPP and fluorescence for different plant functional types. , 2014, , .		0
107	Misión FLEX (Fluorescence Explorer): Observación de la fluorescencia por teledetección como nueva técnica de estudio del estado de la vegetación terrestre a escala global. Revista De Teledeteccion, 2014,	0.6	3
108	Retrieving vegetation clumping index from Multi-angle Imaging SpectroRadiometer (MISR) data at 275m resolution. Remote Sensing of Environment, 2013, 138, 126-133.	11.0	46

#	Article	IF	CITATIONS
109	Gaussian processes uncertainty estimates in experimental Sentinel-2 LAI and leaf chlorophyll content retrieval. ISPRS Journal of Photogrammetry and Remote Sensing, 2013, 86, 157-167.	11.1	124
110	A red-edge spectral index for remote sensing estimation of green LAI over agroecosystems. European Journal of Agronomy, 2013, 46, 42-52.	4.1	214
111	Upward and downward solar-induced chlorophyll fluorescence yield indices of four tree species as indicators of traffic pollution in Valencia. Environmental Pollution, 2013, 173, 29-37.	7.5	89
112	Gaussian Process Retrieval of Chlorophyll Content From Imaging Spectroscopy Data. IEEE Journal of Selected Topics in Applied Earth Observations and Remote Sensing, 2013, 6, 867-874.	4.9	92
113	Estimation of vegetation chlorophyll content with Variational Heteroscedastic Gaussian Processes. , 2013, , .		5
114	Multiple Cost Functions and Regularization Options for Improved Retrieval of Leaf Chlorophyll Content and LAI through Inversion of the PROSAIL Model. Remote Sensing, 2013, 5, 3280-3304.	4.0	110
115	Potential retrieval of biophysical parameters from FLORIS, S3-OLCI and its synergy. , 2012, , .		1
116	Optimizing LUT-based radiative transfer model inversion for retrieval of biophysical parameters using hyperspectral data. , 2012, , .		1
117	Machine learning regression algorithms for biophysical parameter retrieval: Opportunities for Sentinel-2 and -3. Remote Sensing of Environment, 2012, 118, 127-139.	11.0	400
118	Retrieval of Vegetation Biophysical Parameters Using Gaussian Process Techniques. IEEE Transactions on Geoscience and Remote Sensing, 2012, 50, 1832-1843.	6.3	201
119	Mapping Vegetation Density in a Heterogeneous River Floodplain Ecosystem Using Pointable CHRIS/PROBA Data. Remote Sensing, 2012, 4, 2866-2889.	4.0	101
120	Remote Estimation of Crop Chlorophyll Content by Means of High‧pectralâ€Resolution Reflectance Techniques. Agronomy Journal, 2011, 103, 1834-1842.	1.8	26
121	Multioutput Support Vector Regression for Remote Sensing Biophysical Parameter Estimation. IEEE Geoscience and Remote Sensing Letters, 2011, 8, 804-808.	3.1	235
122	Evaluation of Sentinel-2 Red-Edge Bands for Empirical Estimation of Green LAI and Chlorophyll Content. Sensors, 2011, 11, 7063-7081.	3.8	410
123	Spectrodirectional Minnaert- <i>k</i> retrieval using CHRIS-PROBA data. Canadian Journal of Remote Sensing, 2010, 36, 631-644.	2.4	5
124	Merging the Minnaert-\$k\$ Parameter With Spectral Unmixing to Map Forest Heterogeneity With CHRIS/PROBA Data. IEEE Transactions on Geoscience and Remote Sensing, 2010, , .	6.3	13
125	Effects of woody elements on simulated canopy reflectance: Implications for forest chlorophyll content retrieval. Remote Sensing of Environment, 2010, 114, 647-656.	11.0	93
126	Earth system science related imaging spectroscopy—An assessment. Remote Sensing of Environment, 2009, 113, S123-S137.	11.0	382

8

#	Article	IF	CITATIONS
127	Mapping of aggregated floodplain plant communities using image fusion of CASI and LiDAR data. International Journal of Applied Earth Observation and Geoinformation, 2009, 11, 83-94.	2.8	41
128	Fusing Minnaert-k parameter with spectral unmixing for forest heterogeneity mapping using CHRIS-PROBA data. , 2009, , .		1
129	Angular sensitivity analysis of vegetation indices derived from CHRIS/PROBA data. Remote Sensing of Environment, 2008, 112, 2341-2353.	11.0	248
130	Capturing the fugitive: Applying remote sensing to terrestrial animal distribution and diversity. International Journal of Applied Earth Observation and Geoinformation, 2007, 9, 1-20.	2.8	109
131	Grazing lawns contribute to the subsistence of mesoherbivores on dystrophic savannas. Oikos, 2006, 114, 108-116.	2.7	90